Brazilian Journal
of Chemical
Engineering

ISSN 0104-6632
Printed in Brazil
www.abeq.org.br/bjche

Vol. 22, No. 03, pp. 341 - 351, July - September, 2005

SPECIES ACTIVE IN THE SELECTIVE CATALYTIC REDUCTION OF NO WITH *ISO*-BUTANE ON IRON-EXCHANGED ZSM-5 ZEOLITES

M. S. Batista, M. Wallau and E. A. Urquieta-González*

Departamento de Engenharia Química, Universidade Federal de São Carlos,
Cx. P. 676, CEP 13565-905, São Carlos - SP, Brazil.
Phone: (16) 3351-8202; Fax: (16) 260-8286,
E-mail: urquieta@power.ufscar.br

(Received: January 12, 2004 ; Accepted: February 5, 2005)

Abstract - Fe-ZSM-5 catalysts were prepared by ion exchange in aqueous medium or in the solid state and tested in the catalytic reduction of NO with *iso*-butane. X-ray powder diffraction (XRD), atomic absorption spectroscopy (AAS), electron paramagnetic resonance spectroscopy (EPR), X-ray absorption spectroscopy (XANES, EXAFS), temperature-programmed reduction by H_2 (H_2-TPR) and Mössbauer spectroscopy (MÖS-S) were used for sample characterisation. Irrespective of the method used in catalyst preparation, EPR, XANES and MÖS-S showed Fe atoms in the oxidation state of 3+. MÖS-S and H_2-TPR data on Fe-ZSM-5 prepared by ion exchange in the solid state allowed quantification of a lower hematite (Fe_2O_3) concentration and a higher proportion of Fe cations than samples prepared in an aqueous medium. In all the catalysts studied these Fe cations were the active sites in the reduction of NO to N_2 and in the oxidation of *iso*-butane. It is further suggested that coordination of Fe species is another important aspect to be considered in their behaviour.

Keywords: NO reduction; Fe/ZSM-5 catalysts; *Iso*-butane; Mössbauer spectroscopy; XANES/EXAFS.

INTRODUCTION

Industrial processes of external combustion are pointed to as the greatest stationary source of atmospheric pollution, with nitrogen oxide (NO) being one of the most prejudicial pollutants. NO emissions from incineration and thermal units using solid combustibles are higher than 500 ppm and can reach concentrations up to 70,000 ppm, depending on the quality of the combustible used and the industrial activity involved. The selective catalytic reduction of NO to N_2 with hydrocarbons (SCR-HC) under oxidising conditions and using metal-exchanged zeolites has been shown to be an important means of minimisation this pollutant in the atmosphere (Iwamoto and Hamada, 1991). Under industrial operating conditions (presence of water, sulphur oxides and an excess of oxygen), Fe-ZSM-5 zeolites have shown adequate levels of conversion and selectivity for N_2 (Centi and Vazzana, 1999), which are highly dependent on the method used in the preparation of this type of catalyst (Chen and Sachtler, 1998). In spite of the published data on the identification and nature of Fe species formed during preparation, no method enabling their quantification has been reported (Chen et al., 2000). In this context, the aim of this work was to identify and quantify Fe species in Fe-ZSM-5 catalysts prepared by ion

---

*To whom correspondence should be addressed exchange in aqueous solution and in the solid state. The relation of these Fe species to the activity of the catalysts in the reduction of NO to N_2 with *iso*-butane under oxidising conditions was also verified.

EXPERIMENTAL

Fe-ZSM-5 catalysts were prepared by ion exchange in an aqueous medium in N_2 atmosphere using a Na-ZSM-5 zeolite (Si/Al = 11) and a slightly acid solution of $FeCl_2$ (Merck, 0.033 mol/L and pH = 5.5) as zeolite precursor and as a source of Fe cations, respectively. After ion exchange the samples were washed with deionised water and then dried at 110 °C. In the case of preparation of Fe-ZSM-5 catalysts by ion exchange in the solid state, an H-ZSM-5 zeolite (Si/Al = 13) was used as precursor by physically mixing with $FeCl_2$ (Merck, Fe/Al = 0.37) and then thermally treating first at 520 °C under N_2 flow for 2 h and subsequently under air flow for 4 h. To remove the remaining chlorine from the treated solid, it was washed with deionised water and finally dried at 110 °C. Chlorine removal was accompanied by the formation of HCl precipitate during the mixing of a solution of $AgNO_3$ with the filtrate. Washing was stopped when no more AgCl precipitate was observed. A reference sample consisting of a mixture of Fe_2O_3 and Na-ZSM-5 zeolite (Si/Al = 11) was also prepared.

The samples prepared were identified as $|Fe_x|[Si_yAl]$-MFI or $|(Fe_2O_3)_x|[Si_yAl]$-MFI, where x represents the ratio of Fe to Al in the solid, y the ratio of Si to Al in the zeolite and MFI the IZA structure code for the ZSM-5 zeolite (Meier et al., 1996). For the sample prepared by solid-state ion exchange the suffix SE was added.

The catalysts were characterised by XRD, EPR, chemical analysis (AAS), XANES/EXAFS and Mössbauer spectroscopy (MÖS-S). XRD diffractograms were obtained on a Rigaku-Miniflex diffractometer using Cu-? $_{\alpha}$ radiation between 3 to 40° (2Θ) and a goniometer velocity of 2° (2Θ)/min. The EPR analysis was performed with a Bruker ESR-300E spectrometer (IQSC/USP), where the sample under study was put in a quartz tube and the experiment carried out at the temperature of liquid nitrogen. H_2-TPR analyses were carried out at 25 to 800 °C in micromeritics 2705 equipment having a thermal conductivity detector. A cold trap (-50 °C) was placed upstream from the detector to remove the water produced during reduction. In the experiments 100 mg of catalyst (dried at 110 °C), a flow of 30 mL/min of H_2 (5 % in N_2, v/v) and a heating rate of 10° C/min were used. The MÖS-S measurements were carried out at -269 °C, using a 25 mCi ^{57}Co:Rh source. Zero velocity was defined based on the spectrum of metallic Fe, and during the experiment the temperature of the source and the absorber was held constant. The data obtained were processed with the Normos 95 programme. In the XANES and EXAFS analyses the samples were measured by fluorescence at room temperature using synchrotron radiation.

The catalysts were evaluated by the reduction of NO to N_2 using *iso*-butane as reducing agent. Prior to the reaction, the catalysts were activated at 520 °C under air flow during one hour and subsequently cooled to room temperature. The reactor was fed with a gas mixture containing an excess of O_2 (0.30 % NO; 0.24 % *iso*-C_4H_{10} and 2.2 % O_2, balancing in He (v/v)). The reaction temperature was varied from 150 to 500 °C. The used gas space velocity (GHSV) of 42,000 h^{-1} has been calculated considering the total gas flow and a mass of catalyst of 50 mg (previously dried at 110 ºC). To avoid the occurrence of hot spots, the catalyst was mixed with 150 mg of α-quartz. The products of the reaction were analysed on-line by gas chromatography with an FID (Flame Ionization Detector) and a TCD (Thermal Conductivity Detector). One capillary column of Al_2O_3/KCl (30 m × 0.32 mm) and two packed columns, one a Hayesep D (3 m × 1/8") and the other a Chromossorb 102 (5 m × 1/8"), were used.

The activity of the catalysts in the oxidation of *iso*-butane was expressed in terms of total hydrocarbon conversion, taking into consideration the carbon balance during the reaction. The conversion of NO (% X_{NO}) was based on the formation of N_2 according to the equation: X_{NO} (%) = 2 $[N_2] \times 100/[NO]_o$, where $[N_2]$ is the moles of N_2 formed and $[NO]_o$ is the moles of NO fed into the reactor.

RESULTS AND DISCUSSION

Characterisation

Table 1 shows the Fe contents of the prepared catalysts and Figure 1, their XRD patterns. The diffractograms are typical of ZSM-5 zeolites (Treacy et al., 1996) and show a decrease in peak intensity with the increase in Fe content. This decrease is a consequence of the fact that the X-ray absorption coefficient of Fe is higher than that of Na (Cullity, 1967). By XRD no clear evidence of Fe_2O_3 in the analysed catalysts was observed; however, it might be possible that during activation, a small amount of α-Fe_2O_3 (hematite) had formed on the samples. The formation of Fe_2O_3 is suggested due to the slight increase in the reflection around 32.6 °(2Θ) in the diffractogram of activated sample |$Fe_{0.72}$|[Si_{11}Al]-MFI (Figure 1a and Figure 1b). That reflection angle gives the most intense peak in the hematite diffractogram (Figure 1a and Figure 1b). Nevertheless, the identification of hematite is very difficult due to the low intensity of the reflections observed, which are at the sensitivity limit of the equipment, even in the sample discussed above, which is 6.0 % Fe (see Table 1).

The EPR spectra shown in Figure 2 demonstrate that irrespective of method used in catalyst preparation, the values for parameter g corresponding to the main signal on the spectra are in the range of 4.23 to 4.29, which is typical of mononuclear Fe^{3+} cations with a tetrahedral coordination and located at cation-exchange positions in the zeolite (Lee and Rhee, 1999; El-Malki et al., 2000). Values of g between 5 and 7, which correspond to the lowest EPR signal in a magnetic field near 1,000 G observed in all the samples analysed, are also attributed to mononuclear Fe^{3+} ions in a distorted tetrahedral coordination (Lee and Rhee, 1999), possibly as $(Fe{=}O)^+$ cations (El-Malki et al., 2000).

Table 1: Fe content and Fe/Al ratio of |Fe_x|[Si_yAl]-MFI catalysts.

Sample	Exchanges* × time [h]	Fe/Al	Fe content [% (w/w)]
|$Fe_{0.15}$|[Si_{11}Al]-MFI	2 × 6	0.15	1.1
|$Fe_{0.72}$|[Si_{11}Al]-MFI	3 × 24	0.72	5.2
|$Fe_{0.37}$|[Si_{13}Al]-MFI(SE)	1 × 6	0.37	2.8
|$Fe_{0.80}$|[Si_{13}Al]-MFI(SE)	1 × 6	0.80	6.0
|$(Fe_2O_3)_{0.22}$|[Si_{11}Al]-MFI**	-	0.22	1.6

* Number of exchanges
** Obtained by physical mixing

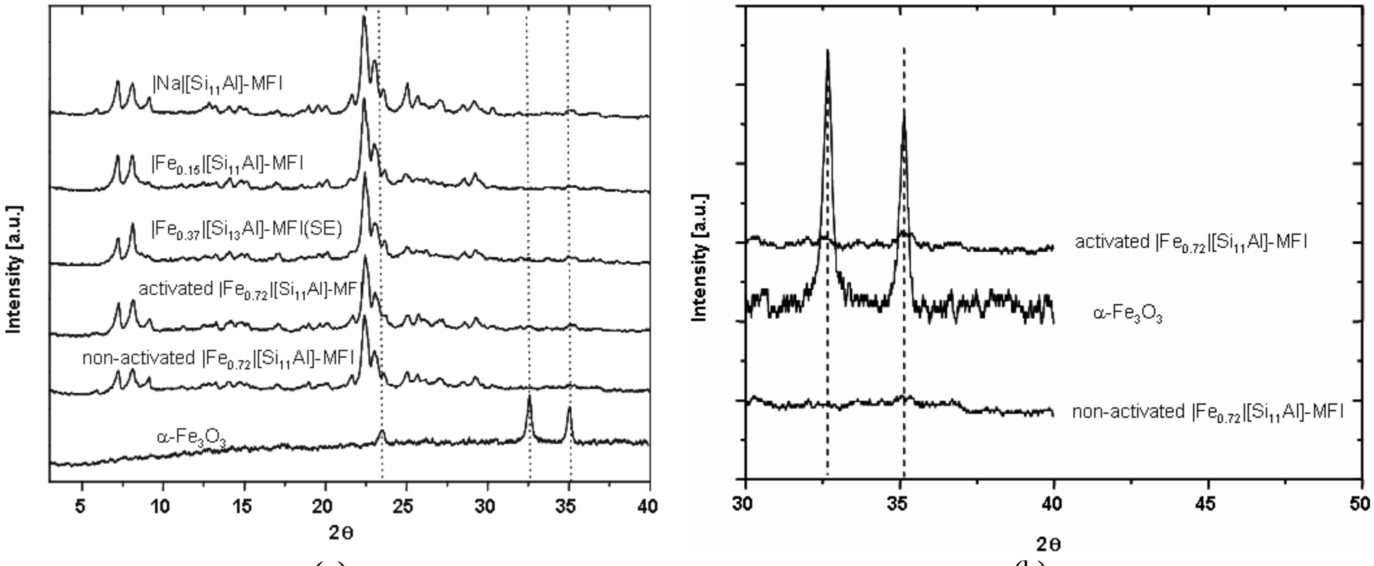

(a) (b)

Figure 1: (a) XRD patterns of precursor |Na|[Si_{11}Al]-MFI, |$Fe_{0.15}$|[Si_{11}Al]-MFI, |$Fe_{0.37}$|[Si_{13}Al]-MFI(SE), activated |$Fe_{0.72}$|[Si_{11}Al]-MFI, non-activated |$Fe_{0.72}$|[Si_{11}Al]-MFI and α-Fe_2O_3; (b) Enlargement of the XRD patterns for activated |$Fe_{0.72}$|[Si_{11}Al]-MFI, α-Fe_2O_3 and non-activated |$Fe_{0.72}$|[Si_{11}Al]-MFI.

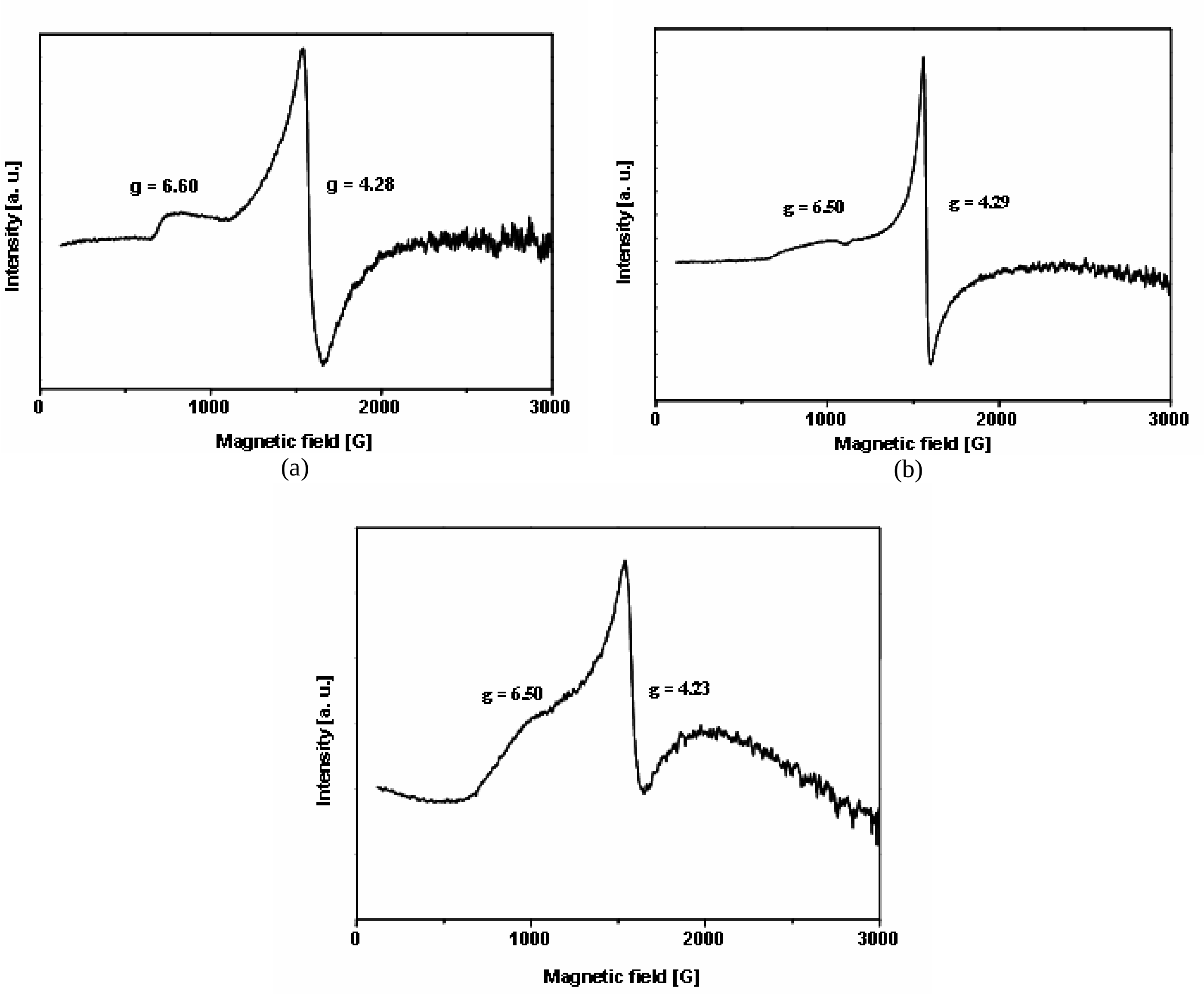

(a) (b)

(c)

Figure 2: EPR spectrum of (a) $|Fe_{0.15}|[Si_{11}Al]$-MFI after ion exchange, (b) $|Fe_{0.15}|[Si_{11}Al]$-MFI after activation at 520°C and (c) $|Fe_{0.37}|[Si_{13}Al]$-MFI(SE).

The difference in the g values can be attributed to the different chemical environments found around the Fe^{3+} ions. In all EPR spectra no signal is observed for Fe species having simultaneously iron ions with oxidation states of 2+ and 3+, which would result in g values between 1.6 and 2.0 (Ramirez et al., 2001).

To serve as a basis for the discussion of XANES analyses of the prepared catalysts, the XANES spectra of reference iron compounds (FeO, FeOOH and Fe_2O_3) are described here. As can be seen, they have a prepeak at around 7120 eV (Figure 3a), which is attributed to the 1s-3d transition (Chen et al., 2000). It should be noted that the intensity of this prepeak is higher for compounds containing Fe^{3+}. However, the peak at 7150 eV, which is more prominent in compounds containing Fe^{2+} than compounds containing Fe^{3+}, cannot be attributed to a particular characteristic of Fe^{2+}, because in this region XANES signals correspond to oscillations in the coordination state of Fe atoms. In Figure 3b it can be observed that irrespective of the method used in sample preparation, XANES spectra of all $|Fe_x|[Si_yAl]$-MFI catalysts have a clear and well-resolved prepeak, which is similar to that seen in the spectra of reference compounds containing Fe^{3+}.

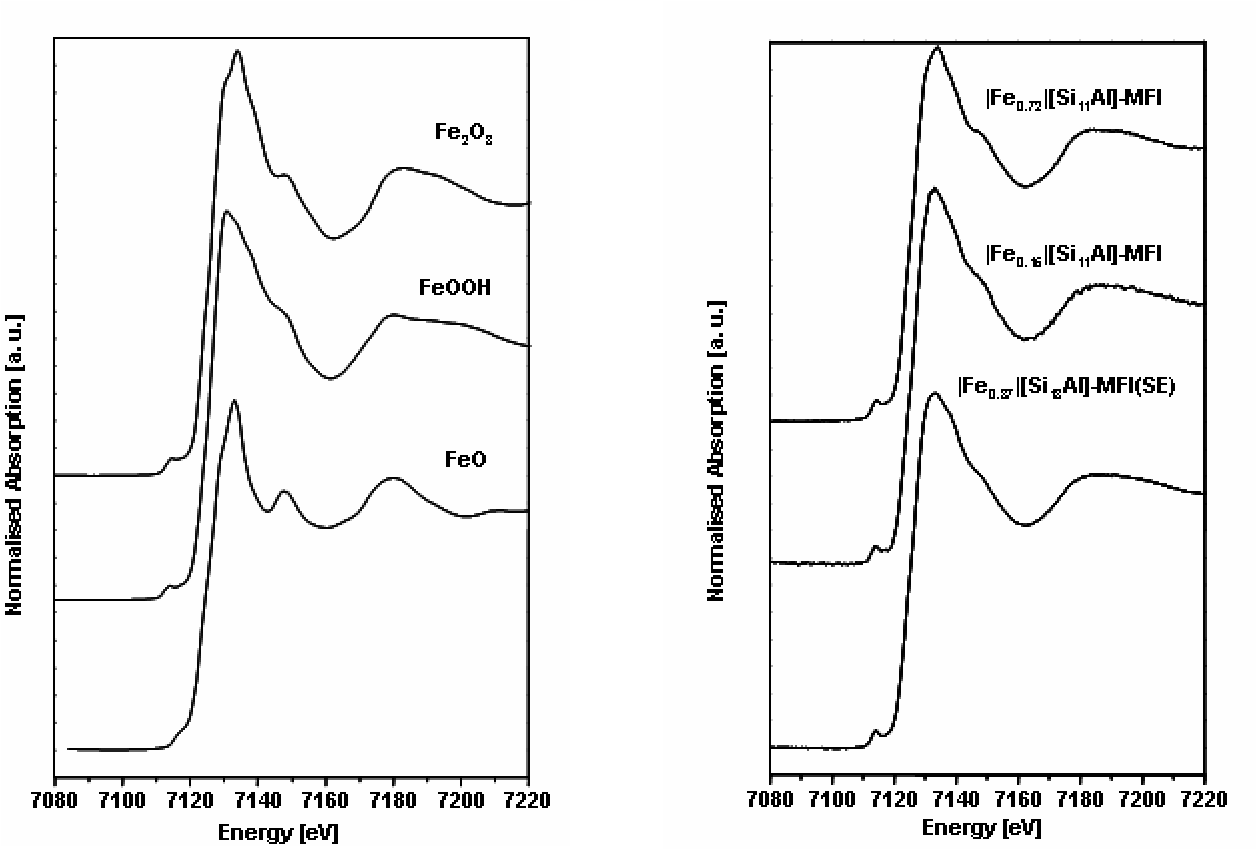

(a) (b)

Figure 3: XANES spectra of (a) reference Fe compounds and (b) activated |Fe$_x$|[Si$_y$Al]-MFI catalysts.

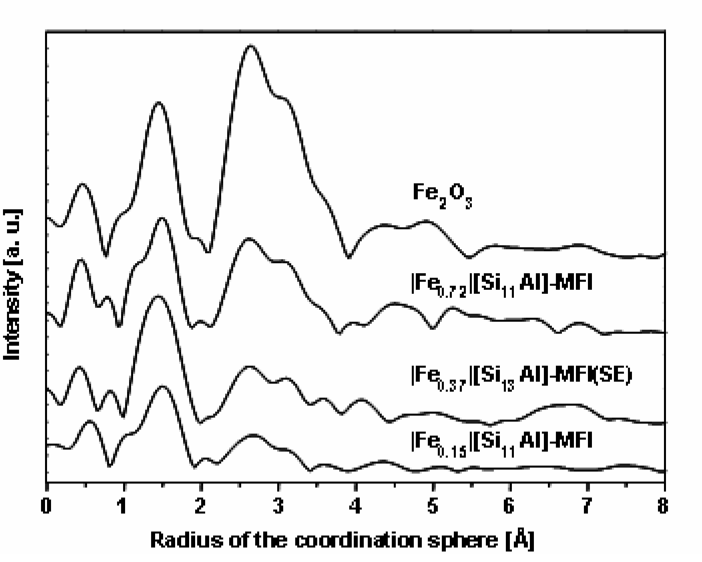

Figure 4: EXAFS spectra of Fe$_2$O$_3$, |Fe$_{0.72}$|[Si$_{11}$Al]-MFI, |Fe$_{0.15}$|[Si$_{11}$Al]-MFI and |Fe$_{0.37}$|[Si$_{13}$Al]-MFI(SE).

The EXAFS spectra for $|Fe_x|[Si_yAl]$-MFI catalysts (Figure 4) are somewhat different from that observed for Fe_2O_3. Although the structural arrangement of the first coordination sphere in Fe_2O_3 (R = 0 – 2 Å) is similar to that in $|Fe_x|[Si_yAl]$-MFI, the intensity of the second coordination sphere (R = 2 – 4 Å) in all $|Fe_x|[Si_yAl]$-MFI samples is lower, indicating that in the latter samples the majority of Fe atoms are highly dispersed (Chen et al., 2000). The increase in the intensity of the second and third coordination spheres (R = 4 – 6 Å) with the increase in Fe content further indicates an increase in the particle size of Fe species. It should be emphasised that for $|Fe_{0.37}|[Si_{13}Al]$-MFI(SE) catalyst, prepared by ion exchange in the solid state, the signal in the first coordination sphere at R = 1 - 2 Å, does not have a shoulder, as seen in the catalysts prepared in aqueous solution, indicating a more homogeneous atomic distribution. As can be further seen in Figure 4, the EXAFS spectrum of $|Fe_{0.37}|[Si_{13}Al]$-MFI(SE) and $|Fe_{0.15}|[Si_{13}Al]$-MFI samples shows a greater diminution in the relative intensity of signals corresponding to the second and the third coordination spheres than that occurring for $|Fe_{0.72}|[Si_{13}Al]$-MFI sample, which have a higher Fe content, thus indicating the formation of smaller particles in the former.

The EPR and XANES results discussed show that in samples prepared in aqueous solution and subsequently activated at 520 °C and also in that prepared in the solid state, all the Fe^{2+} ions were oxidised to Fe^{3+}. It should be kept in mind that during the preparation of $|Fe_x|[SiyAl]$-MFI catalysts in aqueous solution (pH = 5.5), the Fe^{3+} cations formed could precipitate as goethite, i.e. α-FeOOH (Feng and Hall, 1997). During activation of catalysts at 520 °C, goethite is transformed into hematite (α-Fe_2O_3) as schematised by the following equation:

$$2\ \mathrm{FeOOH} \xrightarrow{520^{\circ}\mathrm{C}} \mathrm{Fe_2O_3} + \mathrm{H_2O}$$

Figure 5 shows the H_2-TPR profiles for different $|Fe_x|[Si_yAl]$-MFI samples. It can be seen that they have one reduction peak at around 390°C and other peaks in the range of 450 to 700 °C. In the case of the reference $|(Fe_2O_3)_{0.22}|[Si_{11}Al]$-MFI sample, these peaks can be attributed to the reduction of Fe_2O_3 to Fe_3O_4 (peak at around 390 °C) and to the subsequent reduction of Fe_3O_4 to elemental iron (peak at around 450 to 700 °C), as schematised in the equations below.

$$3\ \mathrm{Fe(III)_2O_3} + \mathrm{H_2} \xrightarrow{390^{\circ}\mathrm{C}} 2\ \mathrm{Fe(II)Fe(III)_2O_4} + \mathrm{H_2O}$$

$$2\ \mathrm{Fe(II)Fe(III)_2O_4} + 2\ \mathrm{H_2} \xrightarrow{450-700^{\circ}\mathrm{C}} 6\ \mathrm{FeO} + 2\ \mathrm{H_2O}$$

$$6\ \mathrm{FeO} + 6\ \mathrm{H_2} \xrightarrow{450-700^{\circ}\mathrm{C}} 6\ \mathrm{Fe^0} + 6\ \mathrm{H_2O}$$

From these equations the theoretical ratio of hydrogen consumed (H_2) per reduced Fe cation (Fe^{3+}) is 1.5, as already observed for $|(Fe_2O_3)_{0.22}|[Si_{11}Al]$-MFI (Table 2).

In the Fe catalysts analysed, isolated Fe^{3+} cations located on ion-exchange sites are reduced to Fe^{2+} at temperatures around 430°C (Chen and Sachtler, 1998; Lobree et al., 1999), while the reduction of isolated Fe^{2+} to elemental Fe^0 occurs at temperatures above 1000°C (Feng and Hall, 1997) and therefore was not observed under the experimental conditions used. Based on the fact that Fe^{3+} cations in neutral oxide species are practically the only completely reduced iron species below 430°C, one can calculate the relative amount of Fe^{3+} in the form of cation charge-compensating species by the following equation:

$$\mathrm{Fe^{3+}}[\%] = \left[1.5 - \left(\mathrm{mols\ of\ H_2\ consumed} \big/ \mathrm{mols\ of\ Fe}\right)_{\mathrm{observed}}\right] \cdot 100\ \%$$

The calculated Fe^{3+} (%) data presented in Table 2 indicate that the relative number of Fe^{3+} cations observed on ion-exchange sites in $|Fe_x|[Si_yAl]$-MFI catalysts prepared in an aqueous medium is around 30 % and did not change with iron content. On the other hand, in the catalysts prepared in the solid state, the relative number of Fe^{3+} cations on ion-exchange sites decreased with the increase in Fe content. However it should be pointed out that for the $|Fe_{0.80}|[Si_{13}Al]$-MFI(SE) sample, the calculated ratio of Fe cations to framework Al (Fe_{cat}^{3+}/Al) is 0.28, which is closer than 0.33, the theoretical Fe_{cat}^{3+}/Al ratio, when all the negative charge of the zeolite framework is being compensated for by isolated Fe^{3+} cations. Therefore, the decrease in the relative amount of iron on ion-exchange sites in the sample discussed is hardly influenced by its high Fe content (6% w/w), which is much higher than its ion-exchange capacity with isolated Fe^{3+} cations (*ca* 2.5% w/w).

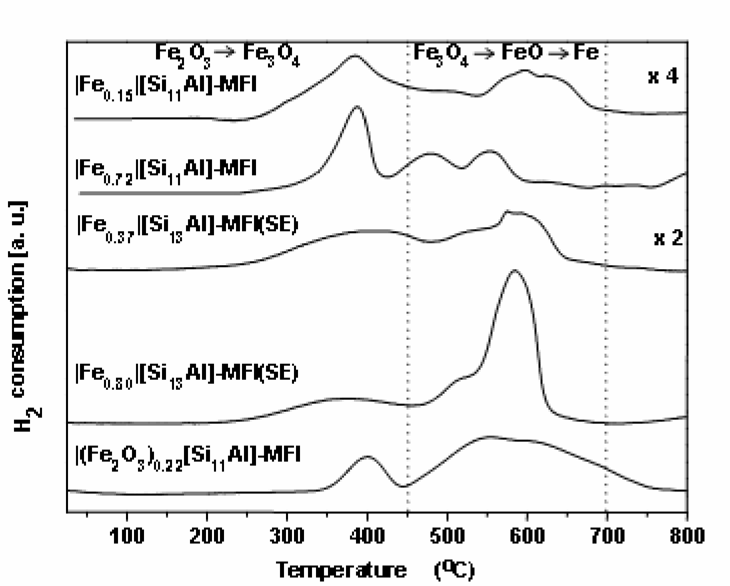

Figure 5: H_2-TPR profiles for $|Fe_x|[Si_yAl]$-MFI catalysts.

Table 2: Ratio of H_2 consumed per iron cation obtained from H_2-TPR data and distribution of cations and neutral extraframework Fe species on the prepared $|Fe_x|[Si_yAl]$-MFI catalysts.

Sample	H_2/Fe	Distribution of Fe species [%]		Fe cation [% w/w]	$[(Fe_{cat}^{3+})^*/Al]^†$
		$(Fe^{3+})^*$	$(Fe^{3+})^{**}$		
$|(Fe_2O_3)_{0.22}|[Si_{11}Al]$-MFI	1.50	0	100	0	0
$|Fe_{0.15}|[Si_{11}Al]$-MFI	1.15	35	65	0.38	0.05
$|Fe_{0.72}|[Si_{11}Al]$-MFI	1.20	30	70	4.56	0.22
$|Fe_{0.37}|[Si_{13}Al]$-MFI(SE)	0.90	60	40	1.68	0.22
$|Fe_{0.80}|[Si_{13}Al]$-MFI(SE)	1.15	35	65	2.10	0.28

*Fe^{3+} in species located on exchangeable sites; †maximum theoretical value = 0.33
**Fe^{3+} in hematite

The Mössbauer spectroscopy data obtained (Figure 6 and Table 3) allowed evaluation of the oxidation state of Fe atoms in the Fe species (Fe^{2+} or Fe^{3+}) and also identification and quantification of the Fe species in the Fe-ZSM-5 catalysts studied. It was necessary to carry out the MÖS-S analysis at -269 °C, because of the occurrence at room temperature of an overlaps of sextets of hematite (α-Fe_2O_3) and goethite (α-FeOOH) with the doublets of the paramagnetic Fe species located on charge-compensating sites in the zeolites (Datye et al., 2000). It can be seen in Figure 6 that the Mössbauer spectra for activated and non-activated $|Fe_{0.72}|[Si_{11}Al]$-MFI and for $|Fe_{0.37}|[Si_{13}Al]$-MFI(SE) are formed of doublets and sextets, corresponding to goethite, hematite and Fe cations on charge-compensating sites. The parameters of the hyperfine structure obtained from these spectra (Table 3) show that the activated $Fe_{0.72}|[Si_{11}Al]$-MFI and $|Fe_{0.37}|[Si_{13}Al]$-MFI(SE) samples have values lower than 1.5 for quadrupole splitting (QS) and values lower than 1 for isomer shift (IS), the latter indicating that these samples contain Fe in the oxidation state 3+ (Niemantsverdriet, 1995). The MÖS-S data corroborate the observations obtained by EPR and XANES and further show the presence of Fe^{2+} in the non-activated $|Fe_{0.72}|[Si_{11}Al]$-MFI sample (Table 3). After ion exchange in the solution of ferric chloride, this latter sample had *ca* 87 % of its Fe atoms as Fe(III) (Fe^{3+} in cations and in goethite) and 13 % as Fe(II). This result shows that during the ion exchange in aqueous solution, even in N_2 atmosphere, the oxidation of Fe^{2+} to Fe^{3+} cannot be avoided. Otherwise, in the activated $|Fe_{0.72}|[Si_{11}Al]$-MFI only Fe in the oxidation state (3+) is observed, providing evidence that during thermal activation all the remaining Fe^{2+} was oxidised into Fe^{3+}. The presence of Fe^{2+} cannot be observed with EPR, because this technique identifies only paramagnetic ions. With XANES, evidence of the presence of Fe^{2+} in the catalyst is not categorical, because this is only supported by the intensity of the prepeak at 7120 eV in the spectra of reference Fe-containing compounds (Figure 3a).

According to the MÖS-S results presented in Table 3, the activated and non- activated $|Fe_{0.72}|[Si_{11}Al]$-MFI and the $|Fe_{0.37}|[Si_{13}Al]$-MFI(SE) catalysts have two types of Fe^{3+} cations on charge-compensating sites, which are tetrahedrally (IS = 0.33 [mm/s]; QS = 1.2 – 1.4 [mm/s]) or octahedrally (IS = 0.3 [mm/s]; QS = 0.3 [mm/s]) coordinated (Delgass et al., 1979). It can also be seen in Table 3, that after activation of the $|Fe_{0.72}|[Si_{11}Al]$-MFI sample the Fe^{2+} cations were oxidised into tetrahedrally coordinated Fe^{3+}, while a small part (*ca* 5 %) of the octahedrally coordinated Fe^{3+} was transformed into hematite. Absolute identification of the Fe species observed by MÖS-S is limited by the difficulty of preparing standards containing the Fe cations probably present in the catalysts. For $|Fe_x|[Si_yAl]$-MFI catalysts prepared in solution, the most probably charge-compensating Fe species are isolated Fe^{3+} and oxo-cations $[HO\text{-}Fe\text{-}O\text{-}Fe\text{-}OH]^{2+}$, the latter transformed into FeO^+ after activation (Chen and Sachtler, 1998). For samples prepared in the solid state, Fe^{3+} and Fe species such as $FeCl_2^+$ or FeO^+ can coexist (Karge and Beyer, 1991).

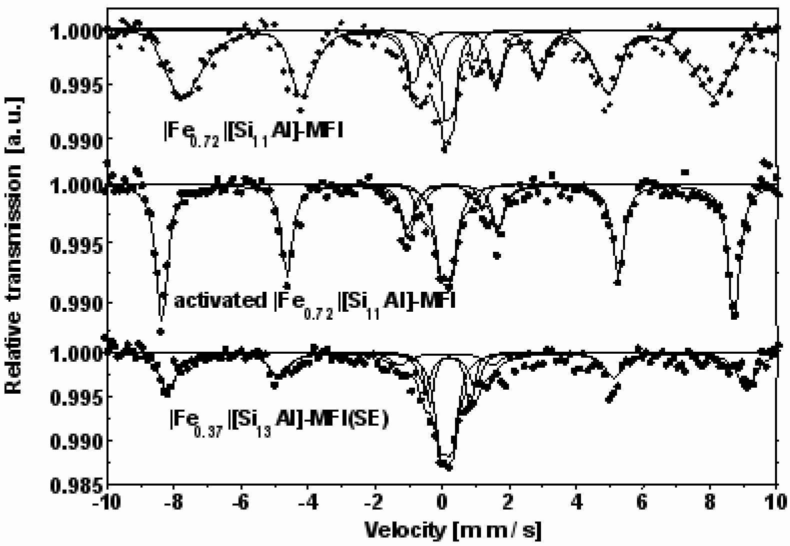

Figure 6: Mössbauer spectra of $|Fe_x|[Si_yAl]$-MFI catalysts measured at -269 °C.

Table 3: Mössbauer data on $|Fe_x|[Si_yAl]$-MFI catalysts obtained at -269 °C.

Sample	IS [mm/s]	QS [(mm/s]	CN	BHF [T]	Area [%]	Fe specie
$|Fe_{0.72}|[Si_{11}Al]$-MFI non-activated	0.30	0.29	6	------	11	Fe^{3+}
	0.33	1.35	4	------	6	Fe^{3+}
	1.45	3.01	-	------	13	Fe^{2+}
	<0.37>	-0.25	-	<49.6>	70	Goethite
$|Fe_{0.72}|[Si_{11}Al]$-MFI activated	0.25	0.30	6	-----	6	Fe^{3+}
	0.34	1.20	4	-----	19	Fe^{3+}
	0.35	-0.20	-	53.0	75	Hematite
$|Fe_{0.37}|[Si_{13}Al]$-MFI(SE)	0.26	0.30	6	------	31	Fe^{3+}
	0.34	1.40	4	------	19	Fe^{3+}
	0.38	0.38	-	53.5	50	Hematite

CN = coordination number; IS = isomer shift related to α-Fe; QS = quadrupole splitting; BHF = magnetic field

Catalytic Activity

In Figure 7 results are shown for the selective catalytic reduction of NO to N_2 and the oxidation of *iso*-butane, used as reducing agent, to CO_2. As can be seen, the conversion of NO (Figure 7a) on the Fe-ZSM-5 catalysts studied reaches a maximum value between 350 °C and 400 °C, behaviour that has also been observed by other authors (Chen and Sachtler, 1998; Chen et al., 1999; Schay et al., 2000).

The lowest activity obtained in both reactions studied on the reference $|(Fe_2O_3)_{0.22}|[Si_{11}Al]$-MFI catalyst indicates that Fe_2O_3 is not active enough for the reduction of NO to N_2 (Figure 7a) and for the oxidation of *iso*-butane (Figure 7b), demonstrating that only Fe^{3+} species on charge-compensating sites are responsible for catalytic activity. Therefore, the $|Fe_{0.72}|[Si_{11}Al]$-MFI catalyst, which has the largest amount of these Fe cations (Table 2), had the greatest activity.

To compare the effects of the nature and the content of the Fe species in the performance of $|Fe_{0.72}|[Si_{11}Al]$-MFI and $|Fe_{0.37}|[Si_{13}Al]$-MFI(SE) catalysts, the former prepared in aqueous solution and the latter in the solid state, data from Mössbauer spectroscopy and from the chemical analysis, are presented in Table 4. As can be seen, both catalysts have practically the same proportion of charge-compensating Fe species, however, the specific activity of these species, calculated as the ratio of mols of NO converted to N_2 per mol of tetrahedrally + octahedrally coordinated Fe cations, was higher for the catalyst prepared in solution (Table 4). This result is consistent with the data published by Long and Yang (2001), who observed that Fe-ZSM-5 catalysts prepared in aqueous solution were more active in the reduction of NO with ammonia than those prepared in the solid state. It can also be seen in Table 4 that the $|Fe_{0.37}|[Si_{13}Al]$-MFI(SE) and $|Fe_{0.72}|[Si_{11}Al]$-MFI catalysts, although having nearly the same quantity of Fe^{3+} cations differ in number of tetrahedrally and octahedrally coordinated Fe^{3+}. As the latter has more of these tetrahedrally coordinated Fe cations, it can be suggested that they are more active than octahedrally coordinated Fe cations, which are predominant in $|Fe_{0.37}|[Si_{13}Al]$-MFI(SE). Given that both of these types of Fe cations have the same specific activity in both catalysts, one can estimate the specific activity of tetrahedrally coordinated Fe^{3+} as 10 [mol $NO_{converted}/Fe_{tetra.}$] and of octahedrally coordinated Fe^{3+} as 3 [mol $NO_{converted}/Fe_{octa.}$].

As the attribution of the Fe^{3+} tetrahedral and octahedral coordination was based only on Mössbauer data, the above suggestion cannot be considered unequivocal; consequently the difference in catalytic activity seen between Fe species having tetrahedral and those having octahedral Fe^{3+} cations must be more explored further.

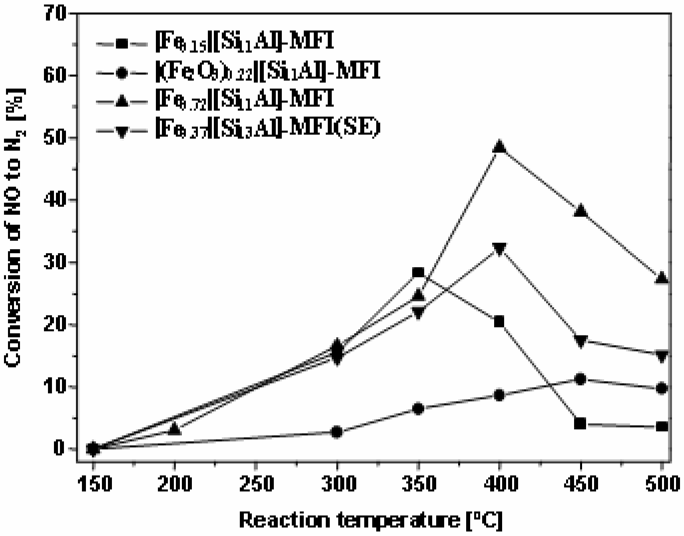

(a)

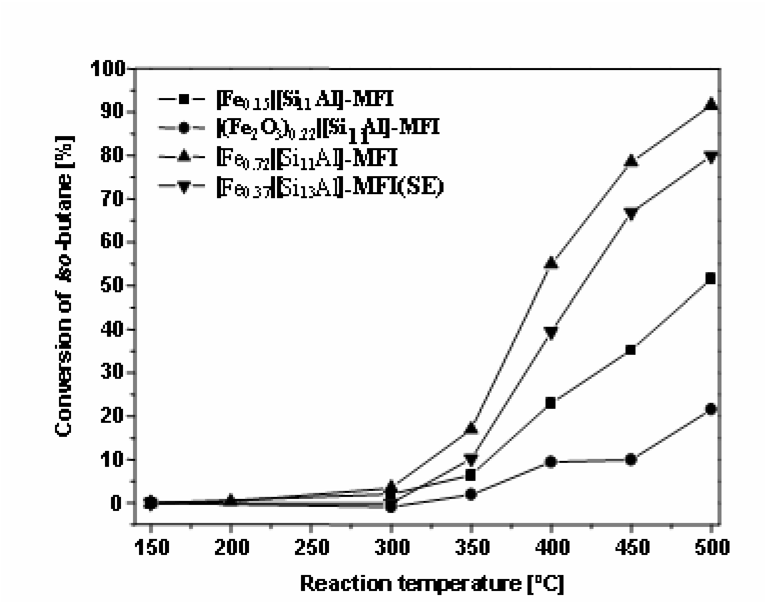

(b)

Figure 7: (a) Reduction of NO to N_2 and (b) Oxidation of *iso*-butane on $|Fe_x|[Si_yAl]$-MFI and $|(Fe_2O_3)_{0.22}|[Si_{11}Al]$-MFI catalysts (GHSV = 42,000 h^{-1}).

Table 4: Distribution of Fe species in $|Fe_x|[Si_yAl]$-MFI catalysts.

Sample	Fe^{3+} on ion exchange sites [% w/w]			Fe^{3+} in hematite [% w/w]	Specific activity**
	total	CN* = 4 $Fe_{tetr.}$	CN* = 6 $Fe_{octa.}$		
$|Fe_{0.72}|[Si_{11}Al]$-MFI (activated)	1.30	0.99	0.31	3.90	8.63
$|Fe_{0.37}|[Si_{13}Al]$-MFI(SE)	1.40	0.53	0.87	1.40	5.95

*CN = coordination number; **calculated as (mols $NO_{converted}$/mols ($Fe_{tetra.}$ + $Fe_{octa.}$) at 400 °C.

CONCLUSIONS

EPR, XANES and MÖS-S results demonstrate that in all the thermally activated $|Fe_x|[Si_yAl]$-MFI catalysts, the Fe was found to be tetrahedrally or octahedrally coordinated with an oxidation state of 3+. In samples prepared in aqueous solution, the oxidation of Fe^{2+} to Fe^{3+} occurred during ion exchange and was completed during activation in air flow at 520 °C. For samples prepared in the solid state the oxidation of Fe occurred during thermal treatment at 520 °C. Based on MÖS-S and H_2-TPR data, it was possible to determine and quantify that some of the Fe species function as charge-compensating species of the zeolite structure, with samples prepared in the solid state having a higher fraction of these. The others form Fe compounds on the zeolite surface.

The activity of these catalysts in the reduction of NO and in the oxidation of *iso*-butane was highly dependent on the content of the Fe cations. The specific activity of the Fe cations in the $|Fe_{0.72}|[Si_{11}Al]$-MFI) catalyst, which are mainly tetrahedrally coordinated, was higher than that of the cations in the $|Fe_{0.37}|[Si_{13}Al]$-MFI(SE) catalyst, which was prepared in the solid state and whose species are mainly octahedrally coordinated. This latter result suggests that coordination of the Fe species is another important aspect to be considered.

ACKNOWLEDGEMENTS

The authors gratefully acknowledge the financial support received from Conselho Nacional de Desenvolvimento Científico e Tecnológico (CNPq/Brazil, grants 477759/2003-3 and 551008/2002-4) for this study. Dr. M. S. Batista thanks Fundação de Amparo à Pesquisa do Estado de São Paulo, Brazil (FAPESP, grant 1998/02495-5) for his doctoral scholarship. The author are also grateful to the National Laboratory of Synchrotron Light (LNLS/Campinas, project XAS 655/2000) and to the Brazilian Center for Physics Research (CBPF)) for conducting the XANES/EXAFS and the Mössbauer spectroscopy analyses, respectively.

REFERENCES

Centi, G. and Vazzana, F., Selective Catalytic Reduction of N_2O in Industrial Emissions Containing O_2, H_2O and SO_2: Behavior of Fe/ZSM-5 Catalysts, Catal. Today, 53, 683 (1999).

Chen, H.-Y. and Sachtler, W.M.H., Activity and Durability of Fe/ZSM-5 Catalysts for Lean Burn NO_x Reduction in the Presence of Water Vapor, Catal. Today, 42, 73 (1998).

Chen, H.-Y., Voskobonikov, T.V. and Sachtler, W.M.H., Reduction of NO_x over Fe/ZSM-5 Catalysts: Mechanistic Causes of Activity Differences between Alkanes, Catal. Today, 54, 483 (1999).

Chen, H.-Y., El-Malki, El-M., Wang, X., van Santen, R.A. and Sachtler, W.M.H., Identification of Active Sites Adsorption Complexes in Fe/MFI Catalysts for NO_x Reduction, J. Mol. Catal. A, 162, 159 (2000).

Cullity, B.D., Elements of X-Ray Diffraction, 3rd Ed., USA: Addison-Wesley (1967).

Datye, A.K., Jin, Y., Manscher, L., Motjope, R.T., Dlamini, T.H. and Coville, N.J., The Nature of the Active Phase in Iron Fischer-Tropsch Catalysts, Stud. Surf. Sci. Catal., 130, 1139 (2000).

Delgass, W.N., Haller, G., Kellerman. R. and Lunsford, J.H., Spectroscopy in Heterogeneous Catalysis, New York: Academic Press (1979).

El-Malki, El.-M., Santen, R.A.V., Sachtler, W.M.H., Active Sites in Fe/MFI Catalysts for NO_x Reduction and Oscillating N_2O Decomposition., J. Catal., 196, 212 (2000).

Feng, X. and Hall, W.K., FeZSM-5: A Durable SCR Catalyst for NO_x Removal from Combustion Streams, J. Catal., 166, 368 (1997).

Iwamoto, M. and Hamada, H., Removal of Nitrogen Monoxide from Exhaust Gases through Novel Catalytic Processes, Catal. Today, 10, 57 (1991).

Karge, H.G. and Beyer, H.K., Introduction of Cations into Zeolites by Solid-state Reaction, Stud. Surf. Sci. Catal., 69, 43 (1991).

Lee, H.-T. and Rhee, H.-K., Stability of Fe/ZSM-5 de-NO_x Catalyst: Effects of Iron Loading Remaining Brönsted Acid Sites, Catal. Lett., 61, 71 (1999).

Lobree, L.J., Hwang, I.-C., Reimer, J.A. and Bell, A.T., Investigations of the State of Fe in H-ZSM-5, J. Catal., 186, 242 (1999).

Long, R.Q. and Yang, R.T., Fe-ZSM-5 for Selective Catalytic Reduction of NO with NH_3: A Comparative Study of Different Preparation Techniques, Catal. Lett., 73, 201 (2001).

Meier, W.M., Olson, D.H. and Baerlocher, Ch., Atlas of Zeolite Structure Types, 4th revised edition, London: Elsevier (1996).

Niemantsverdriet, J.W., Spectroscopy in Catalysis, New York: VCH (1995).

Ramirez, J.P., Mul, G., Kapteijn, F., Arends, I.W.C.E., Ribeira, A. and Moulijn, J.A., Characterization and Performance of Ex-framework Fe/ZSM-5 in Catalytic N_2O Decomposition, Stud. Surf. Sci. Catal., 135, 172 (2001).

Schay, Z., James, V.S., Pál-Bórbery, G., Beck, A., Ramaswamy, A.V. and Guczi, L., Decomposition and Selective Catalytic Reduction of NO by Propane on CuZSM-5 Zeolites: A Mechanistic Study, J. Mol. Catal. A, 162, 191 (2000).

Treacy, M.M.J., Higgins J.B. and von Ballmoos, R., Collection of Simulated XRD Powder Diffraction Patterns for Zeolites, 3rd revised edition, London: Elsevier (1996).